[16]W. A. Harrison, Phys. Rev. 129, 2503 (1963).
[17]J. A. Rayne, Phys. Rev. 129, 652 (1962).
[18]G. B. Brandt and J. A. Rayne, Phys. Rev. 132, 1512 (1963); Phys. Letters 12, 87 (1964).
[19]R. T. Mina and M. S. Khaikin, Zh. Eksperim. i Teor. Fiz. 51, 62 (1966) [Soviet Phys. JETP 24, 42 (1966)].
[20]Obtained from United Mineral and Chemical Corp., New York, N. Y.
[21]Obtained from Wilmad Glass Co., Buena, N. J.
[22]J. F. Gueths, F. V. Burckbuchler, and C. A. Reynolds, Rev. Sci. Instr. 40, 1344 (1969).
[23]F. V. Burckbuchler and C. A. Reynolds, Phys. Rev. 175, 550 (1968).
[24]R. C. Carriker and C. A. Reynolds, Bull. Am. Phys. Soc. 14, 98 (1969).
[25]Throughout this paper we will distinguish $n_3$ from $n_1$ and $n_2$, but not $n_1$ from $n_2$ in the set $(n_1\, n_2\, n_3)$, because of symmetry.
[26]J. B. Goodenough, Phys. Rev. 89, 282 (1953).
[27]J. Friedel, Phil. Mag. 43, 153 (1952); Advan. Phys. 3, 446 (1954).
[28]W. Kohn and S. H. Vosko, Phys. Rev. 119, 912 (1960).

PHYSICAL REVIEW B VOLUME 2, NUMBER 8 15 OCTOBER 1970

# Tunneling Spectroscopy in Degenerate $p$-Type Silicon†

D. E. Cullen,* E. L. Wolf,‡ and W. Dale Compton§
*Coordinated Science Laboratory and Department of Physics, University of Illinois, Urbana, Illinois* 61801
(Received 24 February 1970)

Tunneling in boron-doped $p$-type silicon metal-semiconductor (MS) and metal-insulator-semiconductor (MIS) tunnel junctions has been studied at low temperatures by measuring the derivatives $dI/dV$ and $d^2I/dV^2$ of the current-voltage characteristics as functions of applied bias voltage $V$. The boron impurity concentration of the silicon crystals varied from $6.5\times10^{18}$ to $2.3\times10^{20}\,\mathrm{cm}^{-3}$. Junctions were prepared by evaporating metal contacts onto vacuum- or air-cleaved silicon surfaces. The general features of the tunneling conductance were found to be in qualitative agreement with existing theories of tunneling in semiconductors. Structure in the derivative data resulting from the interaction of tunneling electrons with silicon zone-center optical phonons and boron local-mode phonons has been observed. The optical-phonon line shapes in the most heavily doped MIS units are shown to compare well with the theoretical line shapes in which modifications in the bulk semiconductor states arising from electron–optical-phonon interactions in the semiconductor electrode have been included. The origin of the optical-phonon and local-mode-phonon structure in samples of lower doping is not fully understood.

## I. INTRODUCTION

Tunneling in a wide variety of semiconductor systems has been studied over the past several years. A critical review of much of this work has recently been given by Duke.[1] Of particular importance to the present work are the studies that have been made of processes involving inelastic tunneling, namely, electronic tunneling with the assistance of phonons.[2,3] Such processes are exemplified by a steplike increase in conductance at a bias corresponding to the energy of the participating phonon. These effects are symmetric about zero bias. In a measurement $d^2I/dV^2$ (i.e., $dG/dV$), such effects are seen as antisymmetric peaks.

Wolf[4] first presented data on the tunneling into $p$-type silicon that clearly showed symmetric peaks in $d^2I/dV^2$ at the energies of the zone-center optical phonon. He suggested that such effects arise from a modification in the electronic dispersion relations resulting from electron-phonon interactions. Davis and Duke[5] have shown quantitatively how such modifications can affect the structure in the tunneling conductance. They have made a detailed calculation of the shapes of the lines in $d^2I/dV^2$ versus $V$ that result from these many-body interactions and have compared these calculated line shapes with experimental measurements.

This paper is primarily concerned with the electron–optical-phonon and electron–local-mode-phonon interactions in degenerate $p$-type silicon as revealed in electron tunneling spectra. Preliminary experimental results have already been presented[4,6] as have related theoretical studies.[7,8] We present here more extensive experimental results, with particular attention to the systematic changes that occur as a function of the concentration of the boron dopant. It is shown that the observed line shapes agree with the Davis and Duke formalism only at high doping levels. It is suggested that at the lower doping levels the properties of the barrier begin to dominate and that the

characteristics of it must be considered in determining the nature of the interactions.

Small conductance peaks, about 1 meV wide, and larger conductance minima, typically 5–10 meV wide, were observed at zero bias in the junctions of this experiment. These features are generally categorized as "zero bias anomalies." The wider conductance minimum, which grows in size with decreasing impurity concentration, is a prominent feature of the metal-semiconductor ("MS") units, and will be treated in another paper.[9] The magnetic field dependence of the narrow conductance peaks has been studied by Wolf and Losee.[10] These are interpreted in terms of the Appelbaum theory[11] of magnetic exchange scattering across the tunneling barrier. The required magnetic moments are thought to arise from neutral acceptors localized in the depletion region.

Two factors are worth emphasizing in considering these experiments. First, the cleavage technique used in preparing the junctions insured that the boron density is constant to within a few angstroms of the surface. The problem inherent in fabrication methods involving thermal oxidation and etching of the silicon surface have been avoided. Tests indicate that the present method provides a simple technique for preparing tunnel junctions with reproducible characteristics. Second, a superconductor was used as the metal electrode in all cases. Data are presented *only* if the junctions exhibited the structure of the superconductor for temperatures below the transition temperature of the superconductor.

## II. EXPERIMENTAL CONSIDERATIONS

### A. Junction Fabrication

All of the tunnel junctions whose characteristics are to be described were fabricated from $p$-type silicon single crystals doped with boron. Slices 1 cm thick were sawed from Czochralski-grown crystals with (111) orientation. Variations in resistivity over the entire slice was verified to be never more than a few percent. The boron impurity concentrations $N_a$ were obtained from the room-temperature resistivity versus impurity-concentration data compiled by Irvin.[12]

Briefly, junctions were formed by cutting sample bars from a 1-cm slice, attaching an Ohmic contact, cleaving the silicon bar, and evaporating a metal electrode onto the cleavage plane. Electrical contact was then made to the evaporated metal electrode. In all cases, the junctions were formed on $\{111\}$ crystallographic planes.

Most of the data were obtained with junctions fabricated according to what shall be called the "dot" technique. Rectangular bars, measuring $2\times4\times10$ mm, were sawed from the silicon slices with the [111] axis along the 10-mm direction. All surfaces of the bars were then nickel plated using an electrodeless niclel-plating process.[13] Proper cleansing and etching of the silicon bars in preparation for plating was found to be critical in obtaining low-resistance electrical contacts. After 5 min in the plating solution, the samples were removed and a gold or copper wire was soldered to one of the $2\times4$-mm faces with Ceroseal solder, thereby forming the Ohmic return contact. The resistance of such contacts $R_b$ was determined by soldering contacts to either end of a bar plated only near the ends and measuring the conductance versus bias of the two series contacts. For samples with $N_a$ greater than $1.5\times10^{19}$ cm$^{-3}$, $R_b$ was less than 0.1 $\Omega$. $R_b$ was as high as 5 $\Omega$ for samples with $N_a = 6.3\times10^{18}$ cm$^{-3}$. Since the conductance of the back contact was at least 100 times that of the tunnel junction itself, this undesirable feature of the nickel contacts was not considered serious.

It was desirable to have junctions with resistances greater than 50 $\Omega$ to avoid the distortions of the data accompanying lower resistance junctions (see Sec. II D), and to limit the junction resistance to a few k$\Omega$ since the available signal power depends inversely upon sample resistance. The ambient conditions under which the samples were cleaved were therefore tailored to produce junctions with resistances in this range and to guarantee that the back resistance was negligible compared to the junction resistance.[14] For silicon with $N_a > 10^{19}$ cm$^{-3}$, the junctions were formed by cleaving the bars in laboratory air allowing an insulating layer to grow on the cleavage plane. The exposure time varied from a few minutes to an hour.

Following the oxidation period, the samples were mounted in a diffusion pump vacuum system immediately above an evaporation mask containing an array of small circular holes. At pressures $< 10^{-5}$ Torr, lead or indium was evaporated through the mask onto the cleavage plane to a thickness of 0.5 to 1.0 $\mu$ in 2 to 4 min producing metal dots with areas of 0.0044 to 0.032 mm$^2$, depending upon the mask used.

Samples with concentration $N_a < 1.5\times10^{19}$ cm$^{-3}$ were cleaved in vacuum. This was accomplished with the use of a special cleaving device in the vacuum system.[15] Junctions that were prepared under conditions in which the "MS" interface contamination was minimized (ambient pressure $< 10^{-6}$ Torr, minimal time delay between cleavage and exposure to the evaporating metal, and evaporation rates of 50 Å/sec or greater), were found to be of very low resistance, essentially short circuits. In order to fabricate samples with measurable resistances, it became necessary to increase the time delay and/or increase the pressure. There-

fore, the lower doped samples, $N_a < 1.5\times10^{19}$ $cm^{-3}$, were cleaved in vacuums of $10^{-6}$ to $10^{-5}$ Torr with time delays ranging from a few seconds up to 10 min.

Within a few minutes after removal from the vacuum system, contact was made by lowering a spring-loaded lead or indium tip onto one of the dots. The tip was fashioned by cutting a short length of $\frac{1}{16}$ -in. -diam indium or lead wire to a point using a freshly cleaned razor blade mounted in a microtome. A cold weld was formed between the tip and the dot giving the assembled system some mechanical stability. Contact forces were measured to be between 10 and 100 mg. Delays in making the contact, particularly in high humidity, allowed an oxide layer to form and prevented the formation of the cold weld.

These dot junctions, while possessing some mechanical stability, were quite delicate and great care was required when transferring the assembled junction to the liquid-helium Dewar. Junctions of greater mechanical stability were made by utilizing photoresist methods in making contact to the evaporated metal dots.[16] The initial steps of this process were identical to those of the dot junction process.

After the metal dots had been evaporated onto the cleaved surface of the silicon bar and the sample removed from the vacuum system, the surface was coated with a thin layer of photoresist. The cleavage surface was then examined under a microscope and several dots located on areas free of fracture lines were selected and the areas above these dots exposed to uv light. The photoresist was then developed, producing holes through to the original lead dots, and more lead was then evaporated onto areas above the holes in the photoresist. This second layer of lead was several $\mu$ thick and about $0.5\times1$ mm in area. Contact to the second lead layer was then made by pressure contact. The same spring-loaded tip was used to contact the second lead layer the difference being that, this time, the tip was located at a point off the dot and more pressure was applied. The resulting system proved to be quite stable and it was possible to cycle the junctions between helium temperatures and room temperature repeatedly over an extended period of time without altering the tunneling characteristics. Unfortunately, this process was developed only after most of the data on air-cleaved samples had been accumulated. Nearly all of the vacuum-cleaved samples were fabricated with this dot-photoresist technique.

The dot-photoresist junctions also proved valuable in establishing that the tip used in making contact to the dot samples did not damage the silicon surface and thereby influence the observed phonon line shapes. Data obtained from dot and dot-photoresist samples are in complete agreement with one another, indicating that no such effect is occurring.

Table I contains a listing of the samples from which data will be presented. For each sample, the type of metal contact, room-temperature resistivity, and corresponding boron impurity concentrations are given. The method of construction, i.e., dot or dot-photoresist, is also indicated in the table. For the vacuum-cleaved units, the conditions under which the unit was fabricated, namely, ambient pressure and delay time, are also given. Also indicated in Table I are the calculated values of the Fermi degeneracy $\mu_F$ obtained by assuming parabolic valence bands and effective masses of $m_l = 0.16$, $m_h = 0.4$, and $m_{so} = 0.245$. Contributions to the density of state arising from the spin-orbit split-off band were included for values of $\mu_F$ equal to or greater than the spin-orbit splitting energy of 44 meV.[17] Although the Fermi energies thus calculated will be somewhat in error, particularly for the higher values of $\mu_F$, these values will be sufficient for the present purpose.

In all, the authors measured over 300 junctions.

TABLE I. Sample characteristics.

| $N_a$ ($cm^{-3}$) | Resistivity ($\Omega$ cm) | $\mu_F$ (meV) | Sample No. | Metal electrode | Fabrication technique | Cleavage conditions Vacuum (Torr $\times10^6$) | Time delay (sec) |
|---|---|---|---|---|---|---|---|
| $2.3\times10^{20}$ | 0.00054 | 210 | 57–2 | In | dot | air cleaved | |
| | | | 88 | Pb | dot-photo | air cleaved | |
| $1.2\times10^{20}$ | 0.0010 | 140 | 75 | In | dot | air cleaved | |
| $4.6\times10^{19}$ | 0.0026 | 77 | 81–5 | In | dot | air cleaved | |
| $2.0\times10^{19}$ | 0.0058 | 48 | 82 | In | dot | air cleaved | |
| $1.8\times10^{19}$ | 0.0065 | 45 | 127–2 | Pb | dot-photo | 8 | 600 |
| $1.35\times10^{19}$ | 0.0084 | 37 | 123–2 | Pb | dot-photo | 10 | 300 |
| $1.25\times10^{19}$ | 0.0090 | 35 | 117–1 | Pb | dot-photo | 6 | 300 |
| $9.3\times10^{18}$ | 0.0117 | 29 | 116–1 | Pb | dot-photo | 8 | 300 |
| $6.3\times10^{18}$ | 0.0162 | 23 | 113–2 | Pb | dot-photo | 5 | 15 |

The data from every sample listed in Table I were quite reproducible and every feature of the data discussed in the text was reproduced with several different junctions.

### B. Tunneling Barrier

In the case of air-cleaved samples, the tunneling barrier consists of both the Schottky depletion region in the semiconductor and the oxide layer grown on the surface before evaporation of the metal contact. Because of its complexity, a precise parameterization of the barrier is not feasible. Optical measurements[18] of oxide growth on etched silicon surfaces in room air indicate that thicknesses of about 12 Å are formed in 2 min and that in 3 h this thickness has increased to about 18 Å. The thickness of the oxide film is therefore assumed to be roughly 10 to 20 Å. Metal–silicon dioxide barrier heights have been measured by Deal, Snow, and Mead[19] for several metals; unfortunately neither lead nor indium was studied. The correlation between the electronegativity of the metals and the barrier height suggests, however, that for lead or indium the metal–silicon dioxide barrier is approximately 3.7 eV.

Conductivity measurements[20] on cleaved {111} silicon surfaces indicate that surface states of high density are formed at an energy of $0.60 \pm 0.15$ eV above the valence band when oxygen is absorbed on the cleaved surface. The width $d_s$ of the Schottky depletion layer can be estimated from

$$d_s = (\epsilon\phi_s/2\pi e N_a)^{1/2}\,, \qquad (1)$$

where $\phi_s = 0.60\ \text{eV} + \mu_F$ and $N_a$ is the acceptor concentration near the surface. Barrier widths thus calculated range from about 20 Å for the silicon of highest doping to over 100 Å for the lower doped material. An estimate of the transmission probability of the oxide and Schottky barriers can be readily obtained in the WKB approximation. Such calculations indicate that for $N_a = 2.3\times10^{20}\ \text{cm}^{-3}$ the Schottky barrier contributes negligibly to the junction resistance while at $N_a = 2.0\times10^{19}\ \text{cm}^{-3}$ the transmission probabilities of the oxide and Schottky barriers are of comparable magnitude.

For vacuum-cleaved samples the barrier configuration is less certain. Most of these junctions were prepared under conditions that allowed some contamination of the semiconductor surface prior to the evaporation of the metal contacts. If a sticking coefficient of unity is assumed, then at a pressure of $10^{-6}$ Torr, a monolayer is adsorbed in a few seconds. However, the work of Archer[18] indicates that only about 12 Å or about three monolayers of oxygen are adsorbed on a silicon surface in 2 min at atmospheric pressure. It therefore seems probable that the vacuum-cleaved silicon surfaces have adsorbed no more than a single monolayer. Although these units cannot be described as intimate MS contacts of the type studied by Steinrisser *et al.*,[21] they will be classed as "MS" junctions to distinguish them from true metal-insulator-semiconductor (MIS) junctions.[22] The results of Aspnes and Handler[20] indicate that the adsorption of oxygen greatly alters the surface state density and thus the surface potential. This effect can easily account for the observed change in the resistance of the units cleaved in a partial vacuum.

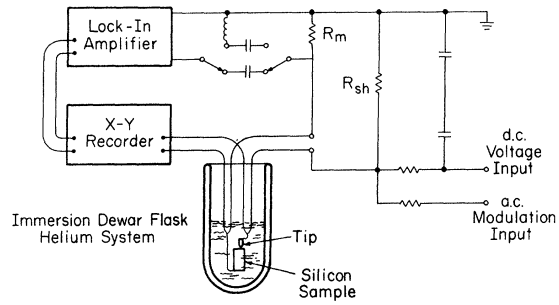


FIG. 1. Simplified schematic of derivative measuring system.

### C. Sample Holders and Cryostat

Dot samples were mounted in one of two special holders designed for these units. A means of adjusting the position of the sample was provided for locating a selected dot on the sample cleavage plane under the spring-loaded tip. In one sample holder the tip was pivoted from a small jewel-mounted axle that was spring loaded with a watch spring. A calibrated germanium resistance thermometer was mounted close to the sample providing accurate temperature sensing. The other system employed a thin cantilevered strip of beryllium copper spring material to provide the spring loading. The indium or lead tip was soldered to the end of the beryllium copper strip.

The sample holder was then attached to the end of a stainless-steel tube and immersed directly in the liquid helium. An electromagnet capable of producing fields up to 5 kG was used for magnetic field measurements.

### D. Measuring System

The ac tunneling conductance $dI/dV$ and its derivative $d^2I/dV^2$ were measured with the system shown in Fig. 1. Derivative techniques are familiar and only a brief description of the measuring circuit is necessary. A 400-Hz signal was applied to the series combination of the tunnel junction and a measuring resistor $R_m$. The modulation was stabilized to better than 1% by the shunt resistor

$R_{sh}$. The ac voltages developed across $R_m$ by the ac current $I(f)$ and the first-harmonic current $I(2f)$ were synchronously detected by a lock-in amplifier and plotted on an $XY$ recorder as a function of applied dc bias voltage $V$. An integrator circuit was used to drive the power amplifier supplying the bias voltage. Sweep rates as low as 0.001 mV/sec were attainable.

The ac currents $I(f)$ and $I(2f)$ at a dc bias $V$ are given by[3]

$$I(f)=\left(\frac{dI}{dV}\right)\left[1+\left(\frac{dI}{dV}\right)R\right]^{-1}\Delta + \text{const}\times\left(\frac{d^3I}{dV^3}\right)\Delta^3+\cdots, \quad (2)$$

$$I(2f)=\frac{1}{4}\left(\frac{d^2I}{dV^2}\right)\left[1+\left(\frac{dI}{dV}\right)R\right]^{-3}\Delta^2 + \text{const}\times\left(\frac{d^4I}{dV^4}\right)\Delta^4+\cdots, \quad (3)$$

where $\Delta$ is the peak value of the ac modulation across $R_{sh}$ and $R$ is the sum of all resistances in series with the tunnel junction. Included in $R$, in addition to $R_m$, are the lead resistance $R_l$, back contact resistance $R_b$, and the spreading resistance $R_{sp}$ of the small metal dot on the silicon surface.[23] The $R_{sh}$ varied between 0.1 and 1.0 Ω and was always less than 1% of the sample resistance. The effect of higher derivatives was minimized by reducing the modulating voltage to the smallest value compatible with the signal-to-noise ratio of the particular junction being studied. For $dI/dV$ measurements this value ranged between 100 μV and 1 mV peak to peak, and for $d^2I/dV^2$ measurements the modulation voltage varied between 1 and 4 mV peak to peak. The term $[1+(dI/dV)R]$ was made as close to unity as possible by minimizing $R$ and controlling the junction fabrication process so as to yield junctions with resistances greater than 50 Ω. $R_m$ was usually 1 Ω and the lead resistance was about 0.5 Ω, so that $R<2$ Ω. (The back contact resistance and spreading resistance together amounted to less than 0.25 Ω for MIS units.) Thus, for a sample with an incremental resistance of 50 Ω at some value of bias $V_0$, the deviations from the true conductance and its derivative introduced by this factor at $V_0$ was 4% for conductance measurements and 10% for second-harmonic measurements. In most cases, the sample resistance was greater than 50 Ω, and the resulting deviations even smaller. This accuracy was deemed sufficient for the present purpose. Also, the position of peaks in $d^2I/dV^2$ is not affected by errors due to higher-order terms in Eq. (3) since these terms will have even symmetry about such peaks and thus will not shift the position of these structures.

It is also important to note that the phonon line shapes would not be noticeably altered by the corrections since the correction factor varies as $[1+(dI/dV)R]^{-3}$, where $(dI/dV)R$ is small (typically less than 0.04), and the change in $dI/dV$ itself over the bias range of the phonon structure is small.

## III. EXPERIMENTAL RESULTS

### A. General Remarks

Figures illustrating experimental data were prepared directly from $XY$ recorder plots. Tracings were made of the recorder plots and these tracings were then photographically reproduced. Since the measuring system yields $I(f)$ and $I(2f)$, it is actually these quantities that appear in the figures. While the true derivaties, $dI/dV$ and $d^2I/dV^2$, could have been obtained by applying the bias-dependent correction factors in Eqs. (2) and (3), these corrections have not been made. As explained in Sec. II D, the parameters of the measuring circuit were chosen to minimize these corrections, and the data are therefore presented as $dI/dV$ and $d^2I/dV^2$ versus $V$.

Positive bias corresponds to raising the Fermi level in the metal with respect to the Fermi level in the semiconductor. Thus, for positive bias the final electron state for a tunneling transition from the metal lies in the silicon valence band. At negative bias, the process may be regarded as tunneling of electrons out of occupied states in the silicon valence band into the metal. Typically, measurements were taken in the range of bias $-100$ mV $< V < 200$ mV. The conductance scales are linear; the vertical scale for $d^2I/dV^2$ data is also linear but of arbitrary magnitude.

Structure resulting from the superconducting energy gap of the metal electrode was observed in all MIS and "MS" functions at temperatures below the critical temperature of the superconductor $T_c$. In the case of the indium, this structure appeared at 3.41 °K within an experimental accuracy of ±0.1 °K. The onset of superconductivity was not observed in lead junctions, since measurements were made only at 77 °K and at temperatures below 4.2 °K. A sensitive comparison of the experimental gap structure can be made with the predictions of the BCS theory by comparing the zero bias differential conductance ratio

$$\left(\frac{dI}{dV}\right)_s \Big/ \left(\frac{dI}{dV}\right)_n$$

with the BCS value.[24] In some cases the correspondence was found to be quite good while other junc-

tions showed large deviations. It was observed, however, that the features of the "good" MIS junctions; namely, phonon line shape, background conductance, etc., showed no correlation with the absence of a detailed agreement between the experimental gap structure and BCS theory.

The phonon structure associated with the superconductivity of the metal electrode was also observed. The 4.4- and 8.5-meV lead phonons are clearly evident in both the $dI/dV$ and $d^2I/dV^2$ data of junctions with lead electrodes. Additional lead phonon structure arising from multiple-phonon processes can be observed out to about 20 meV in the $d^2I/dV^2$ data of these lead junctions. The indium phonon structure is much weaker but can still be observed in the $d^2I/dV^2$ data at about 15 meV.

Tunneling measurements were usually made with the metal electrode in the normal as well as the superconducting states. Indium units were measured at 4.2 and 1.5 °K. Data were taken with the lead in the normal state by applying a magnetic field of a few kG. It was found that fields somewhat greater than the bulk critical field were required to quench the superconductivity, presumably because of fringing of the evaporated dots.[25]

In many cases, samples of a given doping were prepared both with lead and with indium dots. The contacting tip was usually made of the same material as the dots, but in several instances indium tips were used with lead dots. Never was there any evidence of structure in the data related to the type of metal tip, and no structure, other than that due to superconductivity, could be attributed to the metal electrode material.

### B. MIS Junctions

The tunneling characteristics of MIS junctions prepared from the four most heavily doped silicon crystals are shown in Figs. 2–5. The general features of the conductance-versus-bias data are in qualitative agreement with existing predictions for metal-insulator–degenerate-semiconductor contacts. Recent calculations of the conductance of such systems by Chang[26] indicate that, for a semiconductor with a relatively small Fermi degeneracy, the minimum in the conductance should occur at the Fermi energy, and for a more heavily doped semiconductor, the minimum will occur at an energy equal to or smaller than the Fermi energy. The energies of the experimental $dI/dV$ minima are indicated in Fig. 6 and are compared with the calculated values of $\mu_F$. At $N_a = 2.0\times 10^{19}$ cm$^{-3}$, the range of values brackets $\mu_F$. At higher doping, the energies of the experimental conductance minima fall below $\mu_F$, the difference being exaggerated by the aforementioned errors in the calculated values of $\mu_F$. The position of the measured conductance

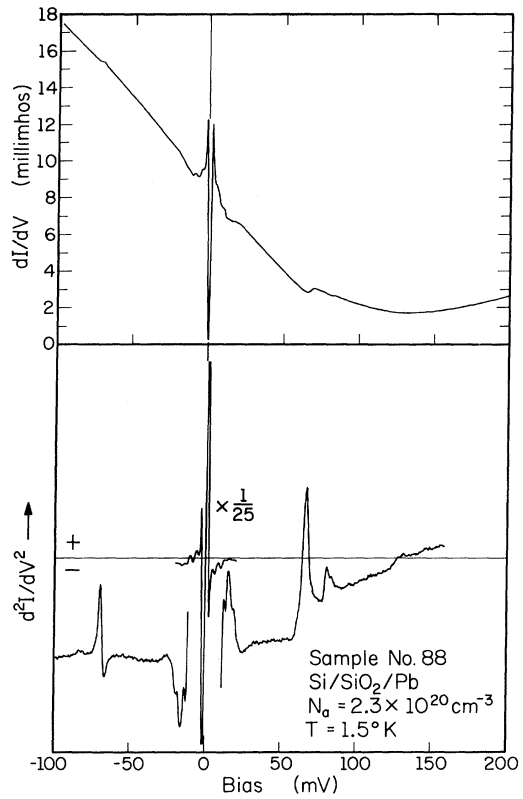


FIG. 2. Tunneling characteristics of silicon MIS junction No. 88 containing $2.3\times 10^{20}$ cm$^{-3}$ boron impurities.

minima therefore conform roughly with Chang's theory. The approximately linear portion of the $dI/dV$ curve of the most heavily doped unit (Fig. 2) in the region eV < 60 meV is in accordance with the conductance versus bias predicted by the elastic specular tunneling model of a MIS junction in which the barrier penetration factor is taken to be a constant.

The interaction of electrons (holes) with bulk semiconductor optical phonons of small wave vector $k$ is observed as structure in $dI/dV$ and $d^2I/dV^2$ at values of applied bias such that $eV \approx \pm\hbar\omega_0$, where $\hbar\omega_0$ is the silicon optical-phonon energy at $k = 0$. Raman scattering experiments at room temperature[27] and helium temperature[28] yield a value of 64.8 eV for this energy.

The position of the positive bias $d^2I/dV^2$ peak has been measured to be $64.2 \pm 0.4$ meV for samples with $N_a = 1.2\times 10^{20}$ and $2.3\times 10^{20}$ cm$^{-3}$. A slight shift in the peak energy is observed with decreasing doping. At $N_a = 2.0\times 10^{19}$ cm$^{-3}$ the peak is located at $64.5 \pm 0.4$ meV. Because of the large Fermi degeneracy of the silicon, it is believed that any differences between the $d^2I/dV^2$ peak energies and the 64.8-meV value from Raman scat-

optical-phonon $d^2I/dV^2$ peak is seen in all "MS" units. In $N_a = 6.3\times10^{18}$ cm$^{-3}$ units, the structure is weak, but nevertheless detectable above the $d^2I/dV^2$ background. If the metal electrode is made superconducting, the peak is sharpened and more readily observed. The increase that occurs in conductance at the optical-phonon energy varies from about 5% in $N_a = 1.8\times10^{19}$ cm$^{-3}$ units to less than 1% in the "MS" junctions of lowest doping. At negative bias the optical-phonon structure is detected only in samples for which $N_a \geq 1.25\times10^{19}$ cm$^{-3}$. The line shape in $N_a = 1.25\times10^{19}$ cm$^{-3}$ junctions is similar to that seen in $N_a = 2.0\times10^{19}$ cm$^{-3}$ MIS units (Fig. 5); i.e., a step down in $d^2I/dV^2$ as the bias is increased in the negative direction. At $N_a = 1.8\times10^{19}$ cm$^{-3}$, the negative bias optical-phonon line shape resembles that seen in $N_a = 4.6\times10^{19}$ cm$^{-3}$ MIS units (Fig. 4). In all cases, the negative bias optical-phonon structure in "MS" junctions is quite weak, making clear identification of the line shape difficult.

The boron local-mode-phonon structure, which was not clearly detectable in the lower doped MIS junctions, is evident in the $d^2I/dV^2$ data of "MS" junctions with $N_a \geq 9.3\times10^{18}$ cm$^{-3}$. While the boron structure was not observed at negative bias in these "MS" units, the positive bias boron peak is seen to be much larger in comparison to the optical-phonon peak than it was in the MIS samples. The $d^2I/dV^2$ boron peak is roughly half as large as the optical-phonon peak. The effect of the superconductivity of the metal electrode on the "MS" phonon line shapes is shown by the dashed lines in Fig. 9.

## IV. DISCUSSION OF RESULTS

For all MIS junctions with $N_a > 2\times10^{19}$ cm$^{-3}$, the interactions between tunneling electrons and optical phonons results in structure in the conductance $dI/dV$ which is approximately *antisymmetric* about zero bias. The corresponding $d^2I/dV^2$ line shapes are approximately *symmetric* about $V = 0$, as seen in Figs. 2–4 and 8. This symmetry is of particular importance for it distinguishes these line shapes from those that would result from phonon-assisted tunneling.

Davis and Duke[4] have calculated the influence of electron interactions with optical phonons on the electronic self-energies in degenerate semiconductors. They have numerically evaluated the effects of such many-body interactions on the tunneling conductance for the case of $p$-type silicon MIS junctions. The resulting theoretical line shape is in qualitative agreement with the structure observed in the $N_a = 2.3\times10^{20}$ cm$^{-3}$ junctions as shown in Fig. 10. Specifically, the calculated $d^2I/dV^2$ line shape has the same symmetry about zero bias, the same relative size of forward to reverse bias structure, and the shape of the theoretical curve

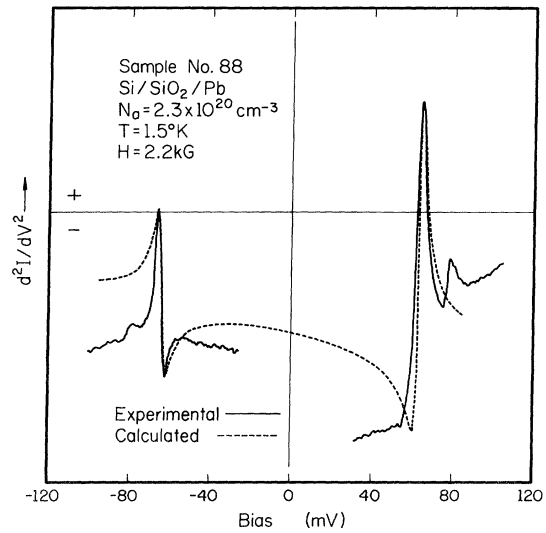


FIG. 10. Comparison of the calculated $d^2I/dV^2$ line shape of Davis and Duke (Ref. 5) with experiment. The parameters of the theoretical curve are given in Ref. 7. Since the calculated background does not accurately depict the experimental background, it was necessary to shift the experimental negative bias phonon structure vertically to coincide with the theoretical curve.

closely resembles the experimental data. The symmetric second-derivative structure is therefore believed to result primarily from an electronic self-energy effect in the semiconductor electrode due to interactions of the tunneling particle and the optical phonons.

Treating the boron impurity as a harmonic oscillator in a degenerate hole (electron) fluid, Davis and Duke[5] also calculated the hole–local-mode-phonon coupling in silicon. They find that the form of the coupling is essentially identical to the hole–LO-phonon coupling in a polar semiconductor. The $d^2I/dV^2$ line shapes resulting from polar coupling (Fig. 8 of Ref. 5) are similar to those obtained with the use of deformation-potential coupling appropriate for silicon (dashed curve in Fig. 10). In both cases, the phonon interaction results in a nearly symmetric second-derivative structure. The symmetric nature of the experimental boron mode $d^2I/dV^2$ structure in the $N_a = 2.3\times10^{20}$ cm$^{-3}$ units therefore suggests that this too is the result of an electron self-energy effect rather than an inelastic phonon emission process.

As the boron impurity concentration is reduced, the MIS optical-phonon line shapes show increasing deviations from the calculated self-energy line shape of Davis and Duke.[5] These variations with doping are particularly evident at negative bias as shown in Fig. 7. Duke and Kleinmann[30] have recently calculated the self-energy line shapes for silicon

of lower doping. Their results indicate that the self-energy $d^2I/dV^2$ line shapes, particularly at negative bias, are not sensitive to the doping of the semiconductor. Therefore, the variations in the experimental $d^2I/dV^2$ structure with doping cannot be attributed to a dependence of the bulk self-energy effect upon impurity concentration.

In view of the concentration dependence of the experimental data and the recent calculation by Duke and Kleinmann,[30] it appears that other effects must be present. One might ask, for example, whether the data can be explained by assuming that both self-energy effects and phonon-assisted tunneling contribute to a significant degree, particularly in the case of the lower doped junctions.

In $N_a = 2.0\times 10^{19}$ cm$^{-3}$ samples, for instance, the silicon Fermi degeneracy is about 48 meV, which is considerably less than the zone-center optical-phonon energy of 64.8 meV. Thus, at a positive bias equal to the phonon energy, electrons tunneling from states near the Fermi level of the metal electrode are tunneling into a state in the forbidden gap of the semiconductor. Emission of an optical phonon may allow this to occur. Self-energy effects at positive bias are expected to be weaker for those cases in which $\hbar\omega_0 > \mu_F$. Since, however, there is no drastic change in the structure of the line at this dopant level, it is likely that inelastic phonon emission plays a reasonably important role in these lower doped junctions.

At negative bias, the situation is somewhat different. The negative $d^2I/dV^2$ peak characteristic of phonon-assisted tunneling was not detected in any of the tunnel junctions of this experiment, and hence there is no evidence for this mechanism at negative bias. Structure resulting from self-energy effects at negative bias is not expected to be sensitive to whether $\mu_F$ is greater or less than $\hbar\omega_0$, as was the case at positive bias. At a negative bias equal to the phonon energy, electrons are tunneling from states deep in the silicon valence band and calculations of the self-energy effect are therefore insensitive to the degeneracy of the semiconductor.[30] The bulk self-energy effect is thus expected to be more evident at negative bias than at positive bias for material in which $\mu_F < \hbar\omega_0$.

Thus, the experimental optical-phonon line shapes in the sequence of MIS samples examined in this work cannot be satisfactorily explained either in terms of the bulk self-energy effect alone or in terms of a combination of bulk self-energy and phonon-assisted tunneling. In addition, even in the most heavily doped units, where the agreement is best between the experimental $d^2I/dV^2$ data and the bulk self-energy line shapes calculated by Davis and Duke,[5] there is a lack of detailed agreement between theory and experiment (see Fig. 10). At positive bias, the sharp negative dip preceding the positive peak is not observed experimentally. At negative bias, the theory predicts a substantial change in the slope of the $dI/dV$ characteristic as the bias is swept from one side of the optical-phonon structure to the other. The experimental data show no such change in slope.

Duke has pointed out that the phonon structure can be influenced by self-energy effects arising from interactions in the barrier region as well as from interactions in the bulk.[31] Such *barrier self-energy effects* might be expected to depend rather strongly upon impurity concentration since various properties of the barrier itself vary with doping. The dependence of the negative bias optical-phonon $d^2I/dV^2$ line shapes upon impurity concentration might then be explained in terms of the dependence of the barrier self-energies upon doping. In particular, it is thought that the self-energies, and hence the line shapes, may be influenced by changes in the screening in the semiconductor depletion region adjacent to the bulk where the free-carrier concentration is nonzero.

Brailsford and Davis[32] have recently shown that structure in the line shapes, similar to that obtained with many-body effects, can occur as the result of a combination of the inelastic process involving phonon emission and interference between the elastic channel and a two-step process involving the excitation and subsequent deexcitation of electrons by phonon emission.

The features of the boron local-mode-phonon structure tend to support the conclusions that interactions in the barrier region and screening are important factors. The symmetry of the boron $d^2I/dV^2$ structure in the $N_a = 2.3\times 10^{20}$ cm$^{-3}$ MIS junctions was used to distinguish that structure from inelastic phonon-assisted tunneling. In the lower doped units, both "MS" and MIS, the boron structure is not observed at negative bias and so an identification on the basis of symmetry about $V = 0$ cannot be made. Even so, the variations in the strength of the effect with impurity concentration and method of device fabrication ("MS" or MIS) allow certain inferences to be drawn.

In the MIS junctions, where the impurity concentration varied between $2.0\times 10^{19}$ and $2.3\times 10^{20}$ cm$^{-3}$, the positive bias boron local-mode-phonon peak was approximately 25% as large as the optical-phonon peak in the most heavily doped units, and the relative size diminished with decreasing boron content until it became nearly undetectable at $N_a = 2.0\times 10^{19}$ cm$^{-3}$. For MIS samples with $N_a < 2\times 10^{19}$ cm$^{-3}$, neither the boron structure nor the silicon optical-phonon structure were unambiguously detected, while both of these phonon peaks were observed in "MS" junctions fabricated from crystals

with the same doping. In "MS" units with $N_a$ between $9.3\times10^{18}$ and $1.8\times10^{19}$ cm$^{-3}$, the boron peak was approximately 40% as large as the optical-phonon peak, and this proportion varied less than 10% over that range of doping. The fact that the phonons can easily be detected in "MS" junctions but not in MIS junctions made from the same semiconductor material is almost certainly related to the properties of the barriers. That the addition of the oxide layer should decrease the transmission of the barrier and make detection of the phonon peaks more difficult is not unexpected. However, not only does the oxide layer cause a rapid decrease in the strength of the phonon structure for silicon with $N_a < 2\times10^{19}$ cm$^{-3}$; but, as is evident by comparing the data from "MS" and MIS junctions in this region of concentration, the optical-phonon and local-mode-phonon structures are not equally affected by the insulating barrier. In MIS units with $N_a = 2.0\times10^{19}$ cm$^{-3}$, the boron phonon peak was not clearly detected, and certainly was less than 10% of the optical-phonon peak. In "MS" units with $N_a = 1.8\times10^{19}$ cm$^{-3}$, the local-mode-phonon peak was 40% as large as the optical-phonon peak and represented an increase in conductance above the conductance at that bias of approximately 2%. This change in the relative size of the boron peak with the type of barrier is indicative of the importance of the barrier in determining the phonon structure. When the oxide is present, the silicon optical-phonon effect is dominant and the interaction with boron local-mode phonons play a secondary role. With no oxide and a barrier consisting of only the Schottky depletion region in the silicon, the boron phonon structure becomes comparable in magnitude to the optical-phonon structure. It seems unlikely that electron-phonon interactions in the semiconductor bulk would be sensitive enough to the nature of the tunneling barrier to produce these effects.

It is concluded, on the basis of these observations, that the interactions giving rise to the optical- and local-mode-phonon structure in the lower doped units occur primarily in the barrier region. Also, the fact that the relative size of the boron peak in the "MS" units remains essentially constant while the boron concentration decreases by a factor of 2 may suggest that screening plays an important part in determining the local-mode-phonon structure. The reduction in screening at lower boron concentrations presumably leads to an increase in the strength of the interaction that is large enough to conterbalance the decrease in density of boron impurity atoms.

It was noted previously that in MIS junctions with $N_a \leq 1.8\times10^{19}$ cm$^{-3}$ the phonon structure was very weak. In view of the fact that the phonons were easily detected in "MS" units with the same doping, the rather sudden disappearance of the phonon structure in the MIS units is not fully understood. At a doping of $N_a = 1.8\times10^{19}$ cm$^{-3}$, the Fermi degeneracy is about 45 meV, and thus close to the spin-orbit splitting energy of 44 meV. If tunneling into the split-off valence band is somehow more probable than tunneling into the light- and heavy-hole bands, then the fact that the phonons seem to disappear when $\mu_F$ becomes less than $E_{so}$ may not be coincidental. More probably, the structure is simply lost in the noise, since MIS units with $N_a \leq 1.8\times10^{18}$ cm$^{-3}$ tended to have higher resistances and, consequently, the data exhibited poorer signal to noise.

## V. SUMMARY

The present measurements demonstrate that electron tunneling is an effective probe of the collective excitation spectra of degenerate semiconductors and of some of the properties of the tunneling barrier. The results presented here suggest that a satisfactory description of the dependence of $dI/dV$ and $d^2I/dV^2$ upon $V$ involves an understanding of the relative importance of three processes, namely, (i) inelastic effects in which phonons are emitted; (ii) many-body effects in the bulk of the semiconductor; and (iii) many-body effects in the barrier, particularly in the Schottky barrier of the semiconductor.

At very high dopant levels, the line shape in $d^2I/dV^2$ is reasonably well fitted by a theory that considers only many-body effects in the bulk semiconductor. At these dopant levels, the many-body effects in the bulk may dominate. It has not been proved, however, that these line shapes cannot also result from many-body effects in or near the barrier.

Since no discontinuity is observed in the shape of the $d^2I/dV^2$ peaks as the dopant level is decreased to a point where $\hbar\omega_0 > \mu_F$, it is suggested that many-body bulk effects cannot dominate the processes at these doping levels. In fact, this suggests that phonon-assisted processes increase in importance as the doping decreases.

At still lower doping levels, in which data on both "MS" and MIS junctions were obtained, the importance of interactions in the barrier becomes evident. In particular, the probability of interactions between tunneling electrons and unscreened ionized boron acceptor impurities is greatly increased at the lower concentrations. Thus, the properties of the barrier begin to dominate and the characteristics of it must be considered.

## ACKNOWLEDGMENTS

The authors are indebted to Professor C. B. Duke and Dr. L. C. Davis for many valuable discussions

of the experimental results and their interpretation. We also thank Professor N. Peacock for the use of his vacuum system and for his assistance in designing the cleavage fixture.

---

†Work supported in part by the Joint Services Electronics Program (U. S. Army, U. S. Navy, and U. S. Air Force) under Contract No. DAAE 07-67-C-019, and in part by Jet Propulsion Laboratory Contract No. 952383.

‡Present address: Research Laboratories Eastman Kodak Co., Rochester, N. Y.

*Present address: United Aircraft Research Laboratories, East Hartford, Conn.

§Present address: Scientific Research Staff, Ford Motor Co., Dearborn, Mich.

[1]C. B. Duke, *Tunneling in Solids* (Academic, New York, 1969).

[2]N. Holonyak, Jr., I. Lesk, R. Hall, J. Tiemann, and H. Ehrenreich, Phys. Rev. Letters 3, 167 (1959).

[3]R. T. Payne, Phys. Rev. 139, A570 (1965).

[4]E. L. Wolf, Phys. Rev. Letters 20, 204 (1968).

[5]L. C. Davis and C. B. Duke, Phys. Rev. 184, 764 (1969).

[6]D. E. Cullen and W. D. Compton, Bull. Am. Phys. Soc. 14, 414 (1969).

[7]L. C. Davis and C. B. Duke, Solid State Commun. 6, 193 (1968).

[8]L. C. Davis, Phys. Rev. B 2, 1714 (1970).

[9]D. E. Cullen, W. D. Compton, and E. L. Wolf (unpublished).

[10]E. L. Wolf and D. L. Losee, Solid State Commun. 7, 665 (1969); D. L. Losee and E. L. Wolf, Phys. Rev. Letters 23, 1457 (1969).

[11]J. Appelbaum, Phys. Rev. 154, 633 (1967).

[12]J. Irvin, Bell System Tech. J. 41, 387 (1962).

[13]M. V. Sullivan and R. M. Warner, Jr., in *Transistor Technology*, edited by F. J. Biondi (Van Nostrand, New York, 1958), Vol. 3.

[14]G. W. Gobeli and F. G. Allen, J. Phys. Chem. Solids 14, 23 (1960).

[15]E. L. Wolf and W. D. Compton, Rev. Sci. Instr. 40, 1497 (1969).

[16]The authors are indebted to Professor N. Peacock for suggesting this method and to L. Schein for assistance.

[17]S. Zwerdling, K. J. Button, B. Lax, and L. M. Roth, Phys. Rev. Letters 4, 173 (1960).

[18]R. J. Archer, J. Electrochem. Soc. 104, 620 (1957).

[19]B. E. Deal, E. H. Snow, and C. A. Mead, J. Phys. Chem. Solids 27, 1873 (1966).

[20]D. Aspnes and P. Handler, Surface Sci. 4, 353 (1966).

[21]F. Steinrisser, L. C. Davis, and C. B. Duke, Phys. Rev. 176, 912 (1968).

[22]The notation "MS" is used here to draw attention to the fact that these junctions have properties resembling MS more closely than MIS, but that the junctions are not free of all interface contamination.

[23]W. Shockley, *Electrons and Holes in Semiconductors* (Van Nostrand, New York, 1950), p. 99.

[24]J. Bardeen, L. Cooper, and J. Schrieffer, Phys. Rev. 106, 162 (1957).

[25]H. L. Caswell, J. Appl. Phys. 32, 105 (1961).

[26]L. L. Chang, J. Appl. Phys. 39, 1455 (1968).

[27]J. H. Parker, Jr., D. W. Feldman, and M. Askin, Phys. Rev. 155, 712 (1967).

[28]G. E. Wright and A. Mooradian, Phys. Rev. Letters 18, 608 (1967).

[29]M. Balkanski and W. Nazarewicz, J. Phys. Chem. Solids 27, 671 (1965).

[30]C. B. Duke and G. G. Kleinmann, Phys. Rev. (to be published).

[31]C. B. Duke (private communication).

[32]A. D. Brailsford and L. C. Davis (private communication).